Dom34:Hbs1 Promotes Subunit Dissociation and Peptidyl-tRNA Drop-Off to Initiate No-Go Decay

Christopher J. Shoemaker, *et al.*

Science **330**, 369 (2010);
DOI: 10.1126/science.1192430

result from the generation of cGMP by cumulus cells and subsequent transfer to oocytes via gap junctions. Most likely, increased oocyte cAMP resulted from higher amounts of oocyte cGMP suppressing oocyte cAMP phosphodiesterase activity.

If the function of the NPPC/NPR2 pathway is to participate in the maintenance of meiotic arrest, then oocytes within Graafian (large antral) follicles of *Nppc* and *Npr2* mutant mice should exhibit precocious gonadotropin-independent resumption of meiosis. Ovaries were removed from 22- to 24-day-old $Npr2^{cn\text{-}2J}/Npr2^{cn\text{-}2J}$ homozygous mutant and $Npr2^{wt}/Npr2^{?}$ control mice 44 hours after injection of equine chorionic gonadotropin (eCG) to promote follicular development and prepared for histological analysis. Because homozygous $Nppc^{lbab}/Nppc^{lbab}$ mice exhibit early postnatal lethality, ovaries of 5-day-old mutant and wild-type control mice were grafted to the kidney capsules of immunodeficient CBySmn.CB17-$Prkdc^{scid}$/J ovariectomized adult mice, a procedure that supports ovarian growth and development. Ovaries were removed 30 days later. The percentages of germinal vesicle (GV) intact (meiosis arrested) and germinal vesicle breakdown (GVBD, meiosis resumed) oocytes in antral follicles were determined by examining serial sections. There were no major morphological differences in ovarian histology in wild-type or mutant ovaries (see low-magnification images in fig. S2). Oocytes in early antral follicles of both mutant ovaries were at the GV stage, the same as in the wild-type controls. However, whereas oocytes in Graafian (late antral) follicles in control ovaries were maintained at the GV stage, 50% of oocytes in $Nppc^{lbab}/Nppc^{lbab}$ and 80% of oocytes in $Npr2^{cn\text{-}2J}/Npr2^{cn\text{-}2J}$ mutant late antral follicles had resumed meiosis (Fig. 3). The finding that the precocious resumption of meiosis phenotype is expressed by only 50% of the oocytes in ovaries of the *Nppc* mutant is likely because $Nppc^{lbab}$ is a hypomorphic mutation, producing a peptide with slight guanylyl cyclase–stimulating activity (*12*). Also, NPPC may circulate in the normal mouse recipients for the mutant ovarian grafts. Cumulus cells in mutant ovaries were tightly packed around maturing oocytes and showed no evidence of cumulus expansion, which would be indicative of gonadotropin-stimulated maturation. Therefore, NPPC and its receptor NPR2 play a major role in maintaining meiotic arrest.

Higher expression of transcripts in cumulus cells than in mural granulosa cells often indicates that oocyte-derived paracrine factors promote cumulus cell expression (*13*). Therefore, the possible role of oocyte-derived paracrine factors in regulating levels of *Npr2* mRNA in cumulus cells was determined. Microsurgical extirpation of oocytes from complexes (oocytectomy, OOX) significantly reduced expression of *Npr2* mRNA in cumulus cells (Fig. 1C). Coculture of cumulus cells with fully grown denuded oocytes (two oocytes/μl) restored levels of *Npr2* mRNA to that observed in intact complexes (Fig. 1C). Therefore, levels of *Npr2* mRNA in cumulus cells are regulated, at least in part, by oocyte-derived paracrine factors. GDF9, BMP15, and FGF8B are paracrine growth factors secreted by oocytes (*14*). Each of these alone only slightly promoted expression of *Npr2* mRNA by cumulus cells in vitro (Fig. 1D). However, combinations of BMP15 + GDF9, BMP15 + FGF8B, or all three proteins promoted levels of *Npr2* mRNA expression in cumulus cells equivalent to those promoted by coculture with cumulus cell–denuded oocytes (Fig. 1D).

Cumulus cells function to support oocyte development, whereas mural granulosa cells have important endocrine functions and become corpora luteal cells after ovulation. Oocyte-derived paracrine factors regulate cumulus cell expression of transcripts at levels different from those in mural granulosa cells (*13*). Thus, the two populations of granulosa cells have distinct roles, and the oocyte profoundly affects the differentiation of cumulus cells to promote its own development. This study demonstrates a complex regulatory network among mural granulosa cells, cumulus cells, and oocytes before the LH surge, one that is essential for maintaining oocyte meiotic arrest.

On the basis of findings presented here and key studies by others, we put forward the following model for the maintenance of meiotic arrest in fully grown mammalian oocytes (Fig. 4). Oocyte cAMP is crucial for maintaining meiotic arrest and is generated by oocyte adenylyl cyclase, which is controlled by the constitutive action of GPR3 and GPR12 via G_s protein (*3*, *4*). Inhibition of oocyte cAMP-phosphodiesterase (PDE3A) activity is essential for sustaining elevated cAMP concentrations (*6*). Cyclic GMP diffuses into the oocyte from companion cumulus cells via gap junctions and inhibits oocyte PDE3A activity and cAMP hydrolysis and maintains meiotic arrest (*7*, *8*). We show here that NPPC produced by follicular mural granulosa cells stimulates the generation of cGMP by cumulus cell NPR2. Oocytes themselves participate in this meiosis-arresting pathway not only by producing cAMP, but also by promoting cumulus cell expression of NPR2 receptors, which generate the cGMP needed to inhibit oocyte PDE3A activity and thereby maintain meiotic arrest.

References and Notes

1. G. Pincus, E. V. Enzmann, *J. Exp. Med.* **62**, 665 (1935).
2. R. G. Edwards, *Nature* **208**, 349 (1965).
3. L. M. Mehlmann *et al.*, *Science* **306**, 1947 (2004).
4. M. Hinckley, S. Vaccari, K. Horner, R. Chen, M. Conti, *Dev. Biol.* **287**, 249 (2005).
5. C. Ledent *et al.*, *Proc. Natl. Acad. Sci. U.S.A.* **102**, 8922 (2005).
6. F. J. Richard, A. Tsafriri, M. Conti, *Biol. Reprod.* **65**, 1444 (2001).
7. S. Vaccari, J. L. Weeks 2nd, M. Hsieh, F. S. Menniti, M. Conti, *Biol. Reprod.* **81**, 595 (2009).
8. R. P. Norris *et al.*, *Development* **136**, 1869 (2009).
9. Y.-Q. Su *et al.*, *Development* **135**, 111 (2008).
10. M. Jankowski *et al.*, *Biol. Reprod.* **56**, 59 (1997).
11. J. Törnell, B. Carlsson, H. Billig, *Endocrinology* **126**, 1504 (1990).
12. T. Tsuji *et al.*, *Biochem. Biophys. Res. Commun.* **376**, 186 (2008).
13. F. J. Diaz, K. Wigglesworth, J. J. Eppig, *J. Cell Sci.* **120**, 1330 (2007).
14. K. Sugiura *et al.*, *Development* **134**, 2593 (2007).
15. T. Pedersen, H. Peters, *J. Reprod. Fertil.* **17**, 555 (1968).

16. We thank G. Cox, T. Gridley, and M. A. Handel for comments in preparation of the manuscript and L. Jaffe for helpful discussions. J.J.E., K.S., and Y.-Q.S. were supported by grants HD23839 and HD21970 from Eunice Kennedy Shriver National Institute of Child Health and Human Development. M.Z. and G.X. received support from National Basic Research Program of China (grants 2007CB947401 and 2006CB504003) and grant 2009SKLAB07-5 from State Key Laboratory for Agrobiotechnology of China. We also thank M. Mazuk, Baylor College of Medicine, for providing GDF9 and BMP15 and M. O'Brien and K. Wigglesworth for technical assistance.

Supporting Online Material

www.sciencemag.org/cgi/content/full/330/6002/366/DC1
Materials and Methods
Figs. S1 and S2
Table S1
References

10 June 2010; accepted 31 August 2010
10.1126/science.1193573

Dom34:Hbs1 Promotes Subunit Dissociation and Peptidyl-tRNA Drop-Off to Initiate No-Go Decay

Christopher J. Shoemaker, Daniel E. Eyler, Rachel Green*

No-go decay (NGD) is one of several messenger RNA (mRNA) surveillance systems dedicated to the removal of defective mRNAs from the available pool. Two interacting factors, Dom34 and Hbs1, are genetically implicated in NGD in yeast. Using a reconstituted yeast translation system, we show that Dom34:Hbs1 interacts with the ribosome to promote subunit dissociation and peptidyl-tRNA drop-off. Our data further indicate that these recycling activities are shared by the homologous translation termination factor complex eRF1:eRF3, suggesting a common ancestral function. Because Dom34:Hbs1 activity exhibits no dependence on either peptide length or A-site codon identity, we propose that this quality-control system functions broadly to recycle ribosomes throughout the translation cycle whenever stalls occur.

The quality of actively translated mRNA is monitored through multiple cellular mechanisms including nonsense-mediated decay (NMD) (*1*), non-stop decay (NSD) (*2*, *3*), and no-go decay (NGD) (*4*). NMD and NSD target transcripts containing premature stop codons or lacking stop codons, respectively. The in vivo targets of NGD are poorly characterized, but appear to include a broad range of stalled translation complexes containing, for example, mRNAs with

inhibitory secondary structure (*4*), chemical damage (*5*), premature stop or rare codons (*4*), or ribosomal defects [a process more broadly referred to as nonfunctional ribosome decay (NRD)] (*6*, *7*).

In *Saccharomyces cerevisiae*, two proteins, Dom34 (Pelota in higher eukaryotes) and Hbs1, were previously implicated in the endonucleolytic event characteristic of NGD (*4*), although neither factor directly catalyzes this cleavage (*8*). These proteins associate both in vivo (*9*) and in vitro (*10*), and although neither protein is essential in yeast, both deletion strains (*DOM34*Δ and *HBS1*Δ) exhibit synthetic growth defects with strains lacking a subset of 40*S* ribosomal subunit proteins (*9*), suggesting involvement in a common process. Dom34 is evolutionarily related to the eukaryotic translation termination factor eRF1, with two notable differences: The central domain of Dom34 lacks the conserved Gly-Gly-Gln (GGQ) motif required for catalysis of peptide release, and the N-terminal domain of Dom34 lacks the Asn-Ile-Lys-Ser (NIKS) motif involved in codon recognition (fig. S1) (*10*–*12*). Hbs1 exhibits substantial sequence identity to eRF3-related guanosine triphosphatases, including eEF1a, which delivers aminoacylated-tRNA to the A site of the ribosome, and Ski7, a factor implicated in NSD in yeast (*3*, *11*). These observations suggested that a Dom34:Hbs1 complex may directly engage the ribosome (similar to eRF1:eRF3) to initiate the events of NGD that ultimately result in mRNA degradation.

To determine whether Dom34:Hbs1 productively interacts with the ribosome, we measured the guanosine 5′-triphosphate (GTP) hydrolysis activity of purified recombinant protein (fig. S2) in the presence or absence of *S. cerevisiae* ribosomal subunits (*13*). Robust hydrolysis occurred only when both Dom34 and Hbs1 were incubated together with both ribosomal subunits (40*S* and 60*S*) (Fig. 1A). This activity parallels the stimulation observed with the homologous translation termination factors eRF1 and eRF3 (*14*). To further characterize the reaction catalyzed by Dom34:Hbs1 on eukaryotic ribosomes, we used an in vitro–reconstituted yeast translation system (*13*, *15*). Programmed complexes were typically composed of 80*S* ribosomes stalled on a defined mRNA with a peptidyl-tRNA in the P site, and either a sense or a stop codon poised in the A site (for "elongation" and "termination" complexes, respectively). We followed the fate of various components by labeling the peptidyl-tRNA either on the peptide moiety (with ^{35}S-methionine) or on the P-site tRNA itself (with ^{32}P at the terminal adenosine) (Fig. 1B).

Radiolabeled dipeptidyl 80*S* termination complexes were treated with either eRF1:eRF3:GTP

Howard Hughes Medical Institute and Department of Molecular Biology and Genetics, Johns Hopkins University School of Medicine, Baltimore, MD 21205, USA.

*To whom correspondence should be addressed. E-mail: ragreen@jhmi.edu

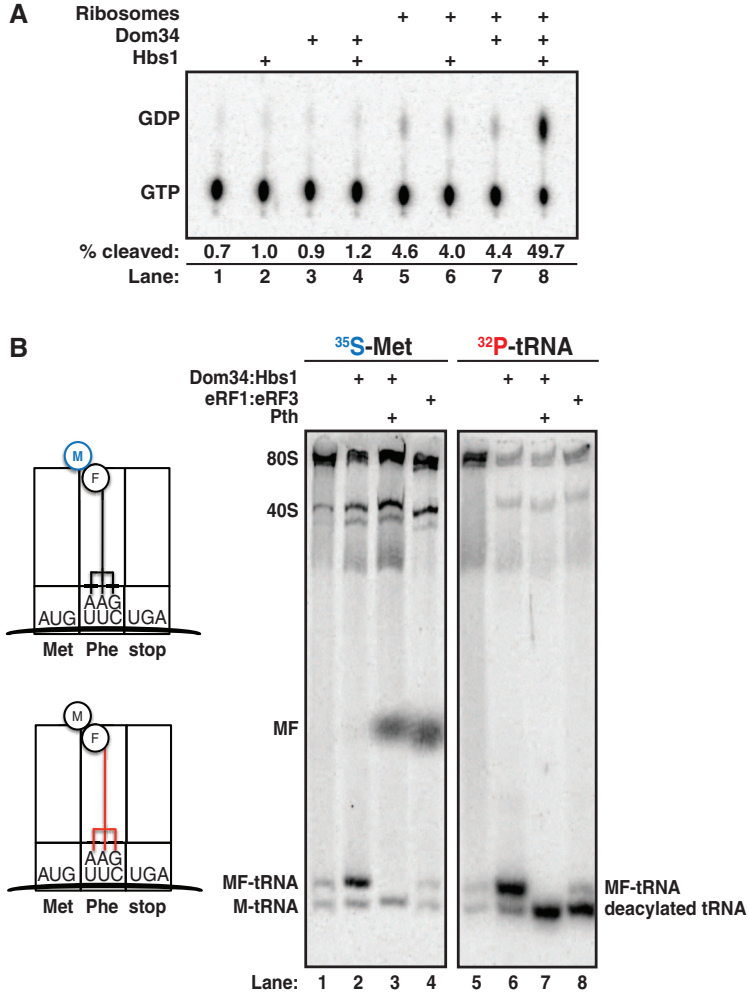

Fig. 1. (**A**) Ribosome stimulation of GTP hydrolysis by Dom34:Hbs1 as visualized by thin-layer chromatogram. (**B**) Native gel analysis of ribosomal termination complexes incubated with indicated components. Stylized diagrams of differentially labeled [^{35}S-Met (blue) or ^{32}P[CCA]-tRNA (red)] ribosome complexes are on the left. Pth, peptidyl-tRNA hydrolase.

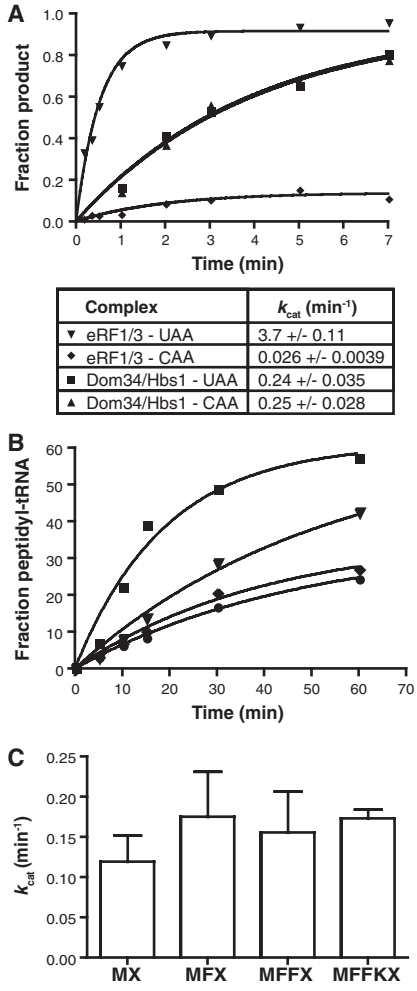

Complex	k_{cat} (min^{-1})
▼ eRF1/3 - UAA	3.7 +/- 0.11
◆ eRF1/3 - CAA	0.026 +/- 0.0039
■ Dom34/Hbs1 - UAA	0.24 +/- 0.035
▲ Dom34/Hbs1 - CAA	0.25 +/- 0.028

Fig. 2. Effects of codon identity and peptide length on Dom34:Hbs1-mediated peptidyl-tRNA release activity. (**A**) Kinetics of release reactions mediated by Dom34:Hbs1 and eRF1:eRF3 on UAA and CAA A-site–programmed ribosome complexes. k_{cat} values are the means ± SD (n = 3). (**B**) Inhibition of Dom34:Hbs1-mediated reaction by a release-defective eRF1 variant [eRF1(AGQ)] on UAA-programmed ribosomes. (■) Dom34/Hbs1 only; (▼) +5 μM eRF1 (AGQ); (◆) +20 μM eRF1 (AGQ); (●) 20 μM eRF1(AGQ) only. (**C**) Rate constants for Dom34:Hbs1-mediated peptidyl-tRNA release on programmed complexes containing Met-tRNA^{iMet}, di-, tri-, or tetra-peptidyl tRNA in the P site (n = 4, ±SD).

or Dom34:Hbs1:GTP, and the products of the reaction were followed by native gel electrophoresis (*16*). eRF1:eRF3:GTP ternary complex promoted the release of two distinct species from 80*S* complexes: ^{35}S-Met-Phe dipeptide (Fig. 1B, lane 4) and ^{32}P-deacylated-tRNA^{Phe} (Fig. 1B, lane 8). By contrast, Dom34:Hbs1:GTP ternary complex promoted the release of a distinct product that migrated at the same position under both labeling conditions (Fig. 1B, lanes 2 and 6), suggesting that it represented intact peptidyl-tRNA. This was confirmed by treatment with recombinant peptidyl-tRNA hydrolase (Pth) (Fig. 1B, lanes 3 and 7), which produced the predicted shifts in product identity (*17*).

The kinetic parameters of the Dom34:Hbs1-promoted reaction were determined with a Pth-coupled reaction and an electrophoretic thin-layer chromatography system (fig. S3) (*18*). Ribosome termination complexes (containing tripeptidyl-tRNA in the P site and a stop codon in the A site) were treated with various factors, and the rate constants for the corresponding reactions were determined. The rate constant for peptide release by eRF1:eRF3 was about 3.7 min^{-1} [as previously reported in the yeast system (*15*)], whereas that of Dom34:Hbs1-promoted peptidyl-tRNA release was slower by a factor of ~15 (Fig. 2A), in a reaction that was dependent on the presence of both factors (fig. S4). Notably, the rate of peptidyl-tRNA hydrolysis by Pth substantially exceeds that of the Dom34:Hbs1-catalyzed peptidyl-tRNA release from the ribosome (fig. S5). As previously observed for eRF1:eRF3 (*19*), catalysis by Dom34:Hbs1 was strongly inhibited in the presence of the nonhydrolyzable GTP analog, GDPNP. The observed inhibition of product formation by both GDPNP and heat inactivation of Dom34:Hbs1 (fig. S6) excludes the uninteresting possibility that nonspecific ribosome dissociation might account for the observed peptidyl-tRNA release.

To test the specificity of these reactions, we compared the reactivity of Dom34:Hbs1 on complexes containing stop (UAA) or non-stop (CAA) codons in the A site. eRF1:eRF3 exhibits a high degree of specificity for stop codons relative to near-stop with rate constants for peptide release differing by about two orders of magnitude (Fig. 2A). By contrast, Dom34:Hbs1 exhibits no specificity for these complexes as the rate constants (and reaction endpoints) are indistinguishable (Fig. 2A). Given the codon-independent nature of the Dom34:Hbs1 reaction, we wanted to confirm that these factors engage the A site of the ribosome. This was accomplished by successfully competing Dom34:Hbs1 activity on termination complexes with increasing amounts of a catalytically inactive eRF1 variant, eRF1(AGQ) (*20*) (Fig. 2B).

Based on the known activities of other A-site–binding factors (e.g., eEF2), we investigated whether Dom34:Hbs1 facilitates a translocation-like process on the ribosome, effectively pushing peptidyl-tRNAs out through the E site. However, because neither length of the peptide (Fig. 2C) nor E-site–bound inhibitors (fig. S7) affected the release reaction, this model seemed unlikely.

A subunit dissociation model was next considered based on the lack of influence of peptide length on the peptidyl-tRNA release reaction, and the likely difficulty of directly releasing such topologically constrained species from intact 80*S* particles. Subunit dissociation was followed with ribosome termination complexes containing either ^{32}P-labeled 40*S* subunits or ^{35}S-Met–labeled peptidyl-tRNA. eIF6, a yeast protein known to bind to the interface region of the 60*S* subunit, served as an anti-association factor that "trapped" dissociation events (*21*, *22*). Indeed, subunit dissociation was promoted by Dom34:Hbs1 (Fig. 3A, lane 5) and correlated nicely with peptidyl-tRNA release activity (Fig. 3A, lane 2). Both reactions were inhibited by the addition of GDPNP (Fig. 3A, lanes 3 and 6) and exhibited similar magnesium dependencies (Fig. 3B). We also followed Dom34:Hbs1-mediated subunit dissocia-

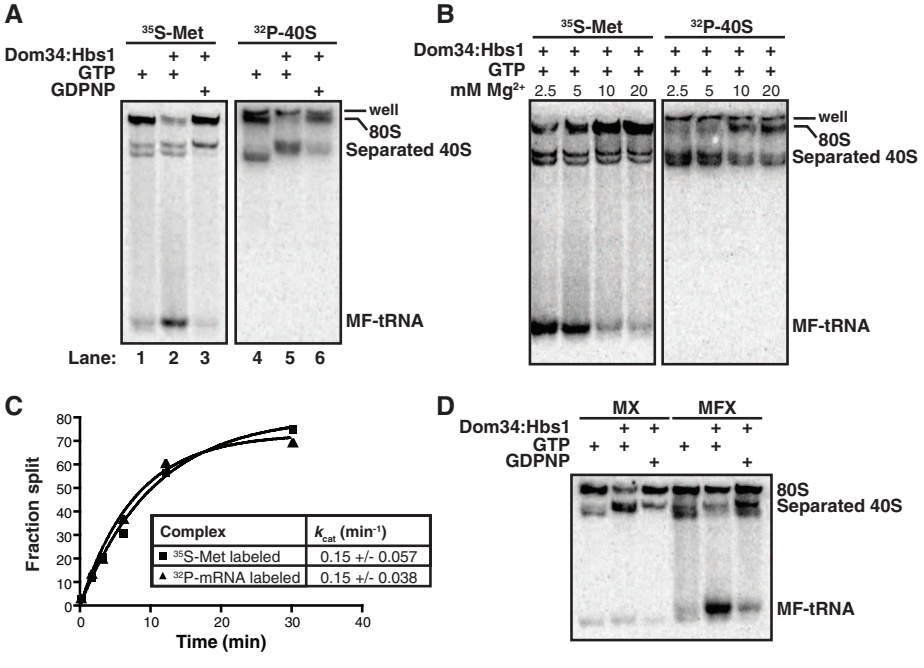

Fig. 3. Dom34:Hbs1 promotes ribosome subunit dissociation. (**A**) Native gel analysis demonstrating GTP dependence of Dom34:Hbs1-mediated products on differentially labeled ribosome complexes. (**B**) Native gel analysis indicating similar magnesium sensitivities for Dom34:Hbs1-mediated formation of peptidyl-tRNA and separation of subunits. (**C**) Rates of peptidyl-tRNA formation and subunit separation are similar. k_{cat} values are the means ± SD (n = 3). (**D**) Native gel analysis reveals distinct products generated from Dom34:Hbs1 treatment of initiation (MX) and elongation (MFX) complexes. Met-tRNA^{iMet} partitions with 40*S* subunits, whereas Met-Phe-peptidyl-tRNA is fully liberated from the ribosome.

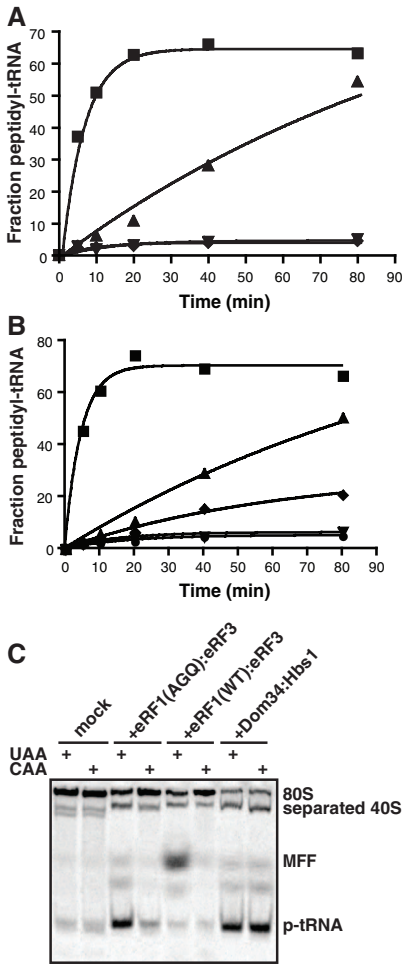

Fig. 4. Intrinsic subunit separation activity associated with eRF1:eRF3. (**A**) Kinetics of peptidyl-tRNA release stimulated by eRF1(AGQ):eRF3. (■) Dom34:Hbs1; (▲) eRF1(AGQ)/eRF3; (▼) mock; (◆) eRF1(AGQ)/eRF3 (GDPNP). (**B**) Stimulation of subunit separation capacity of eRF1(AGQ) by eRF3. (■) Dom34/Hbs1; (▲) eRF1(AGQ)/eRF3; (◆) eRF1(AGQ); (▼) eRF3; (●) mock. (**C**) Native gel analysis of the codon dependence (UAA versus CAA) of eRF1(AGQ):eRF3 recycling activity.

tion using complexes formed with ^{32}P-labeled mRNA and found that the mRNA segregated predominantly with 40*S* subunits (fig. S8), consistent with the previously reported dependence of mRNA dissociation on additional initiation factors (*23*). Additionally, no cleavage of mRNA was observed during Dom34:Hbs1-mediated processes (fig. S9), consistent with an earlier report (*8*).

Because Dom34:Hbs1-driven subunit dissociation and peptidyl-tRNA release are correlated events (Fig. 3, A and B), we sought to determine their order by measuring the rate constants of the two reactions using ribosome complexes containing either ^{32}P-labeled mRNA or ^{35}S-Met–labeled peptidyl-tRNA (Fig. 3C). The observed rate constants for the disappearance of 80*S* ribosomes in a native gel were closely matched (~0.15 min^{-1}) when either the labeled mRNA or peptidyl-tRNA was monitored. These data indicate that subunit dissociation and peptidyl-tRNA formation by Dom34:Hbs1 are tightly coupled to one another, with one likely serving as the rate-limiting step for the other [e.g., (*24*)].

If subunit dissociation occurs first, it seemed possible that an intermediate product might be generated in which subunits have dissociated but peptidyl-tRNA has not yet departed (i.e., peptidyl-tRNA:40*S* subunit conjugates). In a comparison of Dom34:Hbs1 activity on an initiation-like ribosome complex (carrying initiator Met-tRNA^{iMet} in the P site) and on an elongated ribosome complex (carrying Met-Phe-tRNA^{Phe} in the P site), free Met-Phe-tRNA^{Phe} was the predominant product from the Dom34:Hbs1-treated elongated ribosome complex, whereas Met-tRNA^{iMet}–bound 40*S* subunit was the predominant product from the Dom34:Hbs1-treated initiation complexes (Fig. 3D and fig. S10A). The appearance of a Met-tRNA^{iMet}–bound 40*S* complex suggests that subunit separation can take place independently of peptidyl-tRNA release. To confirm that the observed Met-tRNA^{iMet}–bound 40*S* complex represented an authentic stable product of the Dom34:Hbs1-catalyzed reaction, rather than reassociation of Met-tRNA^{iMet} with ribosomes after initial dissociation, we repeated the Dom34:Hbs1-catalyzed reaction in the presence of a large excess of unlabeled Met-tRNA^{iMet} and found that the chase had no effect on the reaction products (fig. S10B). These data are broadly consistent with the previously reported high affinity of 40*S* subunits for Met-tRNA^{iMet} (*25*) and show that the Dom34:Hbs1 complex initially promotes subunit dissociation and that peptidyl-tRNA dissociation typically follows.

Given the structural similarities between Dom34:Hbs1 and eRF1:eRF3, we wondered whether the canonical eukaryotic release factors might also promote subunit separation, independent of peptide release, and thereby contribute to ribosome recycling during termination. Treatment of termination complexes (with ^{35}S-Met–labeled peptidyl-tRNA) with catalytically inactive eRF1(AGQ):eRF3 led to the formation of free peptidyl-tRNA in a reaction inhibited by GDPNP. This activity was distinguished from that promoted by Dom34:Hbs1 only by its slower rate (0.012 min^{-1} versus 0.21 min^{-1}) (Fig. 4A). Like the Dom34:Hbs1-catalyzed reaction, the eRF1(AGQ):eRF3 reaction depended on both protein components for full activity (Fig. 4B). Lastly, we found that eRF1(AGQ):eRF3-mediated peptidyl-tRNA release exhibited robust codon specificity, taking place only when a stop codon was presented in the A site (Fig. 4C).

Canonical recycling, which occurs after termination, involves subunit dissociation, and mRNA and tRNA release, thus allowing for subsequent reinitiation of translation. In bacteria, a specialized ribosome recycling factor, RRF, is central to this GTP-dependent process (*26*). However, in eukaryotes, no RRF has been identified. Our results indicate that eRF1:eRF3 and Dom34:Hbs1 directly destabilize the subunit interface to promote recycling. Although additional factors (including translation elongation factors) appear to promote or accelerate various aspects of recycling in yeast and mammals (*23*, *27*–*29*), our observations could explain why no true RRF homolog is present in eukaryotes where "termination-like" factors instead play the key role in destabilizing the subunit interface. We further argue that Dom34:Hbs1 acts as a specialized recycling factor on malfunctioning ribosome complexes that, for example, do not appropriately engage the next factor in the translation cycle or are inherently defective and thus unable to properly elongate (i.e., NRD) (*6*). Subsequent to Dom34:Hbs1-mediated recycling, kinetic competition between translation reinitiation and mRNA decay (or rRNA decay in the case of NRD) will determine the partitioning of defective RNAs, with the opportunities for degradation accumulating with each passage through the quality-control pathway.

References and Notes

1. S. W. Peltz, A. H. Brown, A. Jacobson, *Genes Dev.* **7**, 1737 (1993).
2. P. A. Frischmeyer *et al.*, *Science* **295**, 2258 (2002).
3. A. van Hoof, P. A. Frischmeyer, H. C. Dietz, R. Parker, *Science* **295**, 2262 (2002).
4. M. K. Doma, R. Parker, *Nature* **440**, 561 (2006).
5. R. Gandhi, M. Manzoor, K. A. Hudak, *J. Biol. Chem.* **283**, 32218 (2008).
6. S. E. Cole, F. J. LaRiviere, C. N. Merrikh, M. J. Moore, *Mol. Cell* **34**, 440 (2009).
7. J. Soudet, J. P. Gélugne, K. Belhabich-Baumas, M. Caizergues-Ferrer, A. Mougin, *EMBO J.* **29**, 80 (2010).
8. D. O. Passos *et al.*, *Mol. Biol. Cell* **20**, 3025 (2009).
9. A. Carr-Schmid, C. Pfund, E. A. Craig, T. G. Kinzy, *Mol. Cell. Biol.* **22**, 2564 (2002).
10. M. Graille, M. Chaillet, H. van Tilbeurgh, *J. Biol. Chem.* **283**, 7145 (2008).
11. G. C. Atkinson, S. L. Baldauf, V. Hauryliuk, *BMC Evol. Biol.* **8**, 290 (2008).
12. H. H. Lee *et al.*, *Mol. Cell* **27**, 938 (2007).
13. M. G. Acker, S. E. Kolitz, S. F. Mitchell, J. S. Nanda, J. R. Lorsch, *Methods Enzymol.* **430**, 111 (2007).
14. L. Frolova *et al.*, *RNA* **2**, 334 (1996).
15. P. Saini, D. E. Eyler, R. Green, T. E. Dever, *Nature* **459**, 118 (2009).
16. M. A. Algire *et al.*, *RNA* **8**, 382 (2002).
17. Z. Vogel, T. Vogel, A. Zamir, D. Elson, *Eur. J. Biochem.* **21**, 582 (1971).
18. E. M. Youngman, J. L. Brunelle, A. B. Kochaniak, R. Green, *Cell* **117**, 589 (2004).
19. E. Z. Alkalaeva, A. V. Pisarev, L. Y. Frolova, L. L. Kisselev, T. V. Pestova, *Cell* **125**, 1125 (2006).
20. L. Y. Frolova *et al.*, *RNA* **5**, 1014 (1999).
21. M. Gartmann *et al.*, *J. Biol. Chem.* **285**, 14848 (2010).
22. K. Si, U. Maitra, *Mol. Cell. Biol.* **19**, 1416 (1999).
23. A. V. Pisarev, C. U. Hellen, T. V. Pestova, *Cell* **131**, 286 (2007).
24. A. Savelsbergh *et al.*, *Mol. Cell* **11**, 1517 (2003).
25. S. E. Kolitz, J. E. Takacs, J. R. Lorsch, *RNA* **15**, 138 (2009).
26. A. V. Zavialov, V. V. Hauryliuk, M. Ehrenberg, *Mol. Cell* **18**, 675 (2005).
27. A. V. Pisarev *et al.*, *Mol. Cell* **37**, 196 (2010).
28. S. Khoshnevis *et al.*, *EMBO Rep.* **11**, 214 (2010).
29. S. Kurata *et al.*, *Proc. Natl. Acad. Sci. U.S.A.* **107**, 10854 (2010).

30. We thank J. Lorsch and his lab members R. Parker and M. Moore for valuable discussions, H. Zaher and N. Guydosh for thoughtful comments on the manuscript, and B. Rogers for cloning and purification of Pth and eIF6.

Supporting Online Material

www.sciencemag.org/cgi/content/full/330/6002/369/DC1
Materials and Methods
Figs. S1 to S10
Tables S1 and S2
References

18 May 2010; accepted 16 August 2010
10.1126/science.1192430

Selection at Linked Sites Shapes Heritable Phenotypic Variation in *C. elegans*

Matthew V. Rockman,[1,2]* Sonja S. Skrovanek,[2,3] Leonid Kruglyak[2,3]*

Mutation generates the heritable variation that genetic drift and natural selection shape. In classical quantitative genetic models, drift is a function of the effective population size and acts uniformly across traits, whereas mutation and selection act trait-specifically. We identified thousands of quantitative trait loci (QTLs) influencing transcript abundance traits in a cross of two *Caenorhabditis elegans* strains; although trait-specific mutation and selection explained some of the observed pattern of QTL distribution, the pattern was better explained by trait-independent variation in the intensity of selection on linked sites. Our results suggest that traits in *C. elegans* exhibit different levels of variation less because of their own attributes than because of differences in the effective population sizes of the genomic regions harboring their underlying loci.

Some phenotypes exhibit abundant heritable variation and others almost none. As heritable variation is the raw material for adaptation, the forces that shape its distribution across traits are a central concern of evolutionary genetics (*1*). Among wild strains of the partially